

1 **Population dynamics of the cosmopolitan eukaryotic picophytoplankton *Bathycoccus***
2 **during seasonal blooms in the bay of Banyuls sur Mer (North Western Mediterranean**
3 **sea)**

4 Martine Devic*¹, Cédric Mariac², Valérie Vergé¹, Philippe Schatt¹, Louis Denu¹, Jean-Claude
5 Lozano¹, François-Yves Bouget*¹ and François Sabot*²

6 Author affiliations :

7 ¹ Laboratoire d'Océanographie Microbienne (LOMIC), CNRS/Sorbonne Université,
8 UMR7621, Observatoire Océanologique, 66650 Banyuls/mer, France.

9

10 ² Diversité, adaptation et développement des plantes (DIADE), UMR 232 IRD/UM/CIRAD,
11 Centre IRD de Montpellier, 911 avenue Agropolis, BP 604501, 34394, Montpellier Cedex 5,
12 France.

13 * corresponding authors : martine.devic@obs-banyuls.fr; francois-yves.bouget@obs-
14 banyuls.fr; francois.sabot@ird.fr

15

16 *Running head* : Markers of genetic diversity in *Bathycoccus*

17 *Key words* : Phytoplankton, *Bathycoccus*, intra-specific diversity, marker, bloom

18

19 **word count for Abstract, Introduction, Materials and Methods, Results and Discussion :**

20 **7569 words**

21

22

23 **Abstract (251 words)**

24 Although *Bathycoccus* is one of the most abundant picophytoplankton, little is known about
25 the genetic diversity underlying its adaptation to ecological niches. In this study, the diversity
26 of *Bathycoccus* populations during their annual bloom in the Mediterranean bay of Banyuls
27 France was assessed by an INDEL based approach. Oxford Nanopore Technology (ONT) was
28 used to characterise structural variants (SV) among the genomes of *Bathycoccus* sampled
29 from geographically distinct regions in the world ocean. Markers derived from INDEL were
30 validated by PCR and sequencing in the world-wide strains. These markers were then used to
31 genotype 55 *Bathycoccus* strains isolated during the winter bloom 2018-2019 in Banyuls.
32 With five markers, eight Multi Loci Genotypes (MLG) were determined, two of which
33 represented 53% and 29% of the isolates. Physiological studies confirmed that isolates are
34 phenotypically different, cells isolated in February growing better at low temperature than
35 those isolated in December. When tested on environmental samples, two diversity markers
36 showed a similar allele frequency in sea water as in individual *Bathycoccus* strains isolated at
37 the same period. We conclude that these markers constitute a resource to identify the most
38 abundant variant alleles in a given bloom. A follow-up on three consecutive blooms revealed
39 differences in allele abundance during the course of a bloom, particularly at initiation, and
40 between years. In addition to *Bathycoccus prasinos*, two other species of *Bathycoccus* were
41 identified including the recently described species *B. calidus* and a novel species *B. catiminus*,
42 suggesting that species diversity of the genus *Bathycoccus* may be underestimated.

43

44 **Introduction (929 words)**

45

46 Marine phytoplankton, including picoalgae, is responsible for a large fraction of primary
47 production ([Li et al., 1983](#)). In temperate regions, the abundance and diversity of the
48 phytoplankton is often seasonal and occurs in bursts, as algal blooms. Per se, blooms have a
49 large impact on global primary production and therefore the understanding of the effects of
50 ocean warming on phytoplanktonic blooms is of the utmost importance.

51 In the bay of Banyuls, Mamiellophyceae (*Bathycoccus* and *Micromonas*) bloom yearly from
52 November to April. Previous work centred on the occurrence and abundance of different
53 species during the course of a bloom showed that *Bathycoccus* was one of the most abundant
54 species ([Lambert et al., 2019](#)). *Bathycoccus* together with *Ostreococcus* and *Micromonas* are
55 picoalgae in the order of Mamiellales belonging to the green lineage. Widely distributed from
56 the equator to arctic and antarctic poles with a marked seasonality in temperate and polar
57 regions ([Joli et al., 2017](#), [Tragin et al., 2018](#), [Lambert et al. 2019](#), [Leconte et al., 2020](#)), this
58 cosmopolite presence illustrates a high capacity for adaptation to a wide range of contrasting
59 environments. The highly reproducible yearly reoccurrence in the Banyuls bay during the last
60 decade ([Lambert et al., 2019](#)) also raises the question of the persistence of a *Bathycoccus*
61 population adapted to the bay or of a variation of the population structure each year. In
62 addition, since outside of the bloom period, Mamiellales are virtually absent from the bay, is
63 the *Bathycoccus* bloom initiated by an uptake of resident “resting cells” in the sediment or by
64 a fresh input carried by North western Mediterranean currents along the gulf of Lion? At
65 present no resting stages that can act as inoculum of subsequent blooms have been described
66 for *Bathycoccus*.

67 Assessing interspecies diversity uniquely underestimates the diversity of the populations.

68 Equally, a single isolate cannot represent the diversity of a population. Since natural selection

69 acts on variation among individuals within populations, it is essential to incorporate both
70 intra- and inter-specific trait variability into community ecology (Violle et al. 2012). Raffard
71 et al (2019) demonstrated that intraspecific variation has significant ecological effects across a
72 large set of 52 species, confirming a previous estimate based on a more restricted species set
73 (Des Roches et al., 2018). Furthermore, it has been shown that diversity within species is
74 rapidly decreasing, making them more homogenous and highlighting the need to preserve
75 intraspecies variations (Des Roches et al. 2018) since intra-species diversity reinforces the
76 overall population stability in the face of environmental change.

77 In most studies, phytoplankton diversity and abundance have been primarily determined by
78 microscopy at species level and by metabarcoding on the nuclear or plastidial 18/16S rRNA
79 gene. It is now imperative to incorporate intraspecific variability into population studies.

80 In diatoms, intraspecific variation has been shown to play a key role in the responses of the
81 species to several important environmental factors such as light, salinity, temperature and
82 nutrients (Godhe et al. 2017). Modelling efforts indicate that this variation within species
83 extends bloom periods and likely provides sufficient variability in competitive interactions
84 between species under variable conditions. The intraspecific variation most likely corresponds
85 to optimal fitness in temporary microhabitats. This rich intraspecific genetic diversity allows
86 for the possibility of local adaptation and for differentiation in important physiological
87 characteristics that produces local populations that are exceptionally fit and competitive in
88 their respective local habitat.

89

90 To date, very little information is available on intraspecies diversity of Bathycoccaceae with
91 the exception of *Ostreococcus* (Blanc-Mathieu et al, 2017). *Bathycoccus* may be divided in
92 two clades or species, the polar and temperate *Bathycoccus prasinus* type B1 genome
93 (Moreau et al. 2012; Joli et al. 2017) and the tropical *Bathycoccus calidus* type B2 genome
94 (Vannier et al. 2016; Limardo et al. 2017; Bachy et al. 2021). Thus the cosmopolitan nature of

95 Bathycoccus from poles to equator might be due to the combination of the B1 and B2 clades
96 or species. Several studies suggest that previously recognized cosmopolitan species are
97 actually composed of multiple populations or even multiple species (Kashtan et al., 2014).
98 Genotypes or species can either replace each other temporally (but with overlap) as in the
99 case of the marine diatoms *Pseudo-nitzschia multistriata* (Tesson et al., 2014) and
100 *Skeletonema costatum* (Gallagher, 1980) or co-exist sympatrically as in the freshwater
101 *Asterionella formosa* (Van Den Wyngaert et al., 2015). Furthermore, the frontier between
102 variant genotype and species is thin and knowledge will be gained by whole genome
103 sequencing of a large number of accessions. Read et al. (2013) reveal a pan genome of the
104 coccolithophore *Emiliana sp* suggesting that what was previously considered a single
105 species, is actually composed of multiple species.

106 One of the major challenges in the study of marine phytoplankton intraspecies variation is the
107 difficulty to isolate individuals in sufficient number for classical diversity analysis
108 (microsatellites : Srivastava et al. 2019, mitochondrial DNA : Galtier et al. 2009, chloroplastic
109 DNA : Wheeler et al. 2014, nuclear Simple Sequence Repeats SSR, Single Nucleotide
110 Variant (SNV). Microsatellites have been described in some diatoms (Tesson et al. 2011) but
111 not yet in Mamiellales. Meta-ribosomal barcoding has opened the access to massive data in
112 time and space and has accelerated the study of natural communities, inter-species co-
113 occurrence and potential biotrophic interactions. Now it is imperative to develop new tools to
114 study intraspecies diversity in environmental samples. To address this problem, we combined
115 an efficient method to isolate Mamiellales with whole genome sequencing by Oxford
116 Nanopore Technology (ONT) in order to identify Structural Variants (SV) in the Bathycoccus
117 genome. Diversity markers designed from INDEL were used to genotype Bathycoccus
118 accessions and populations from environmental samples.

119

120 **Materials and Methods (885 words)**

121 *Algal strains and culture conditions*

122 World-wide Bathycoccus strains were obtained at the Roscoff Culture Collection (RCC)
123 centre: RCC4222, RCC5417, RCC1613, RCC685, RCC1615, RCC1868, RCC4752 and
124 RCC716. The strains were cultivated in 100 mL flasks in filtered artificial seawater (24.55 g/
125 L NaCl, 0.75 g/L KCl, 4.07 g/L MgCl₂ 6H₂O, 1.47 g/L CaCl₂ 2H₂O, 6.04 g/L MgSO₄ 7H₂O,
126 0.21 g/L NaHCO₃, 0.138 g/L NaH₂PO₄ and 0.75 g/L NaNO₃) supplemented with trace metals
127 and vitamins. Cultures were maintained under constant gentle agitation in an orbital platform
128 shaker (Heidoph shaker and mixer unimax 1010). Realistic sunlight irradiation curves were
129 applied during the light period in temperature-controlled incubators (Panasonic MIR-154-
130 PE).

131

132 *Cell isolation*

133 Surface water was collected at 3 meters depth at SOLA buoy in Banyuls bay, North Western
134 Mediterranean Sea, France (42°31'N, 03°11'E) approximately every week from December 2018
135 to March 2019, November 2019 to March 2020 and October 2020 to April 2021. Two ml aliquots
136 were used to determine the quantity and size of phytoplankton by flow cytometry. For the
137 bloom 2018/2019, 50 ml was filtered through a 1.2-µm pore-size acrodisc (FP 30/1.2 CA-S cat
138 N° 10462260 Whatman GE Healthcare Sciences) and used to inoculate 4 culture flasks with
139 10 ml of filtrate each. The sea water was supplemented by vitamins, NaH₂PO₄, NaNO₃ and
140 metal traces at the same concentration then artificial sea water (ASW), antibiotics
141 (Streptomycine sulfate and Penicillin at 50 µg/ml) were added in half of the cultures. The
142 cultures were incubated under light and temperature conditions similar to those at sampling
143 date for 3-4 weeks. The presence of picophytoplankton was analysed by a BD accury C6 flow
144 cytometer. In general, superior results were obtained without antibiotics. Cultures containing

145 at least 90% of picophytoplankton with only residual nanophytoplankton were used for
146 plating on agarose. Colonies appearing after 10 days were hand picked and further cultured in
147 2 ml ASW in deepwell plates (Nunc, Perkin Elmer, Hessen, Germany) for 10 days. Cells were
148 cryopreserved at this stage. Circa 500 clones were cryopreserved. At the same time, DNA
149 extraction and PCR were performed in order to identify *Bathycoccus* clones.

150 *DNA extraction, genome sequencing, assembly and PCR amplification*

151 For PCR analysis, total DNA was extracted from 4 ml *Bathycoccus* cell cultures according to
152 the Plant DNA easy Qiagen protocol. For whole genome sequencing by Oxford Nanopore
153 technology (ONT), DNA was extracted by a CTAB method from 100 ml culture principally
154 based on Debladis et al. (2017). ONT libraries were barcoded using the Rapid Barcoding
155 Sequencing (SQK-RBK004) and deposited on R9.4 flow cell. For environmental samples, 5
156 litres of seawater at SOLA 3 meters depth were passed through 3 micron and 0.8 micron pore
157 filters. DNA from cells collected on the 0.8 micron filters were extracted using the Plant DNA
158 easy Qiagen protocol with the addition of a proteinase K treatment in the AP1 buffer. PCR
159 was performed using the Red Taq polymerase Master mix (VWR) with the required primers
160 ([Supplemental data 2](#)) and corresponding DNA. For sequencing, the PCR products were
161 purified using the NucleoSpin Gel and PCR Clean-up kit (Macherey-Nagel reference
162 740609.50) and the filtrate was sent to GENEWIZ for Sanger sequencing.

163 Raw ONT Fast5 data were basecalled using Guppy 4.0.5 (<https://nanoporetech.com>) and the
164 HAC model, and QC performed using NanoPlot 1.38.1 ([De Coster et al. 2018](#)). All reads with
165 a QPHRED higher than 8 were retained and subject to genome assembly using Flye 2.8
166 ([Kolmogorov et al. 2019](#)) under standard options. Raw assemblies were then polished with 3
167 turns of standard Racon ([Vaser et al. 2017](#)) after mapping of raw reads on the previous
168 sequence using minimap2 (-ax map-ont mode; [Li et al. 2021](#)). Final scaffolding was
169 performed using Ragoos 1.1 ([Alonge et al. 2019](#)) upon the original *B. prasineos* reference

170 genome (GCA_002220235.1, [Moreau et al. 2012](#)). Final QC of assemblies was performed
171 using QUAST 5.0 ([Mikheenko et al. 2018](#)).

172 *Relative allelic abundance in environmental samples*

173 Amplifications were performed twice with a difference of 2 cycles in order to obtain clear
174 bands on ethidium bromide stained agarose gels for each sample. Similarly the gels were
175 photographed after different exposure times in order to obtain a non-saturated image for each
176 sample. Relative abundance of each variant within the same DNA sample was performed
177 using ImageJ software Analyse Gel.

178 *Determination of Growth Rates*

179 For each culture condition the cell number was determined by flow cytometry daily, for 10
180 days. The growth rate in batch culture was determined as $\text{Ln}(N)/dT$, where N is the cell
181 concentration per ml and T the time (days). The maximal growth rate (μ_{max}) was determined
182 according to [Guyon et al. \(2018\)](#) on a graph expressing the neperian logarithm of cell
183 concentration as a function of time of culture. M_{max} corresponded to the slope of the linear
184 part of the growth curve (i.e., excluding the lag phase and the stationary phase).

$$185 \quad \mu_{\text{max}} = \frac{\text{Log}(N_{\text{fmax}}) - \text{Log}(N_0)}{\text{Log}(2) \times T}$$

186

187 *Measurement of photosynthetic capacities*

188 Cultures were acclimated to the temperature and light rhythm and intensity for 7-10 days
189 before subculturing at 10^6 cells /ml in triplicates. After 3-4 days of growth, the photosynthetic
190 activities were recorded with PHYTO-PAM-II (Walz). After 20 min in obscurity, the samples
191 were transfer into the PHYTO-PAM and Fv/Fm, ETR_{max} and NPQ were measured.

192

193 *Ultrastructure of Bathycoccus species determined by transmission electronic microscopy*

194 Cells were prepared according to [Chrétionot-Dinet et al. \(1995\)](#). Thin sections were stained

195 with uranyl acetate and lead citrate and observed with a 7500 Hitachi transmission electronic
196 microscope.

197

198 **Results (3164 words)**

199 *Search for intraspecies diversity markers*

200 With the aim to differentiate *Bathycoccus* isolates, we undertook a search for genetic
201 determinants of diversity. Since only two Mediterranean strains were available in the Roscoff
202 culture collection at the beginning of the project, we examined the world-wide diversity of
203 *Bathycoccus* and selected the most geographically dispersed accessions (**Supplemental Table**
204 **1**). *Bathycoccus* cells differ at the genome level and can be differentiated in two types, B1 and
205 B2 genomes ([Limardo et al. 2017](#)). Roughly the accessions possessing the B1 genome run
206 along a latitude gradient from the Baffin bay (67°) to the Mediterranean sea (40°). The most
207 tropical accession, RCC716 from the Indian Ocean (-14°) was not included in this analysis
208 since it has a B2 genome, recently described a novel species named *Bathycoccus calidus*
209 ([Bachy et al. 2021](#)). Oxford Nanopore Technology (ONT) was used to sequence the genome
210 of 7 B1 accessions (RCC4222 clone replaces RCC1105 which was lost). After *de novo*
211 assembly, each genome was compared to the reference genome of Banyuls isolate RCC1105.
212 There were some large chromosomal rearrangements but for the design of diversity markers,
213 we only considered INDEL inferior or equal to 2 kb within regions mapping on the RCC1105
214 genome. The number and size of INDEL are detailed in **Table 1**. The goal was to identify
215 INDEL instead of SNP (Single Nucleotide Polymorphism) that could be used to genotype the
216 strains directly by PCR.

217 *Validation of sequence variations in the genomes of world-wide *Bathycoccus**

218

219 Putative markers were selected on several criteria. The insertion should be found at the same
220 or close location in the genome of at least three accessions and of different sizes in at least
221 two genomes, preferably three. In addition, the size of the amplified fragment should be
222 between 200 bp and 2 kb (this size restriction reduced the mean number of insertions from 88
223 to 35, [Table 1](#)) and sufficiently different among the genomes of the accessions to be
224 unambiguously visualised on agarose gel after amplification with a single set of primers. The
225 aim of this drastic selection was to identify the most divergent markers among the largest
226 available genetic diversity of *Bathycoccus* with the expectation that some of this variation
227 would be found in local communities of *Bathycoccus* in the Banyuls bay. Only five candidate
228 markers met these criteria and were experimentally tested. For two markers targeting
229 variations of the number of amino acid repeats in open reading frames, primers positioned at
230 proximity of the repeats did not produce a single amplicon and these two predictions from
231 ONT could not be validated nor invalidated. Marker on chromosome 15 (the number of
232 repeats in a zinc finger protein), marker chromosome 14 (variation in repeat number in a
233 flavodoxin-like protein) and marker chromosome 1 (insertion and deletion into the promoter
234 of *yrdC* gene) were validated ([Table 2](#)). To increase the number of markers, the striking
235 insertion of 1.5 kb into the promoter of the clock gene *TOC1* on chromosome 17 was
236 included even though its diversity was below three ([Table 2](#)). The fifth marker was selected as
237 marker of the Big outlier Chromosome (BOC) on chromosome 14 ([Moreau et al. 2012](#)).

238

239 Typical PCR results for the 5 validated diversity markers are presented in [Figure 1](#).

240 The detailed description of each marker is provided as [supplementary data 1](#).

241 *Bathy01g04300* encodes a *yrdC* domain-containing protein of unknown function. In
242 *Escherichia coli*, *yrdC* binds preferentially to double-stranded RNA, consistent with a role of
243 the protein in translation ([Teplova et al. 2000](#)). A diverse organisation was identified in the

244 promoter region of Bathy01g04300 in comparison to the reference genome RCC1105 and
245 was visualised by amplification with primers MDB33 and MDB34 (Figure 1, Table 2,
246 Supplemental data 1A). This set of primers showed marked differences in its amplification
247 success among the accessions indicating important nucleotide variations.

248 The intergenic region upstream Bathy17g01510 encoding an homolog of TOC1 involved in
249 the control of circadian rhythm was not similar in all accessions. A 2.2 kb insertion was
250 identified in RCC1613, RCC1615 and RCC4752 after amplification, whilst the other
251 accessions were similar to RCC4222 (Figure 1, Table 2, Supplemental data 1B).

252 Bathy03g02080 encodes a protein containing a flavodoxin-like domain, a flavin
253 mononucleotide (FMN)-binding site and 6 imperfect repeats of 25 amino acids. In
254 comparison to RCC1105, ONT sequencing revealed insertions of 147 bp in RCC4222, 74 bp
255 in RCC1613 and 375 bp in RCC685, while RCC1868 and RCC4752 were unchanged. These
256 predictions verified by PCR and sequencing confirm that substantial INDEL can also occur
257 within coding regions (Figure 1, Table 2, Supplemental data 1C).

258 Bathy15g02320 encodes a protein with Zinc Finger repeats (ZF) of a greater length in Arctic
259 (9ZF) and RCC685 (7ZF) than in RCC4222 (6ZF). Primers were designed to amplify the
260 array of ZF motifs (Figure 1, Table 2, Supplemental data 1D). Since MDB68 and MDB69 did
261 not amplify a single fragment in RCC5417 and RCC1868, the corresponding region was
262 obtained by the ONT data (Table 2). Zinc finger C2H2 protein are numerous (53 genes) and
263 highly conserved in the Bathycoccus reference genome (Moreau et al. 2012).

264 Bathy14g30100 encodes the protein containing a TIM domain found in the protein Timeless
265 involved in circadian rhythm control in Drosophila (Sehgal et al. 1995). This gene is located
266 in the BOC region of chromosome 14, a part of the chromosome potentially involved in
267 mating type (Moreau et al. 2012). The ORF of TIM was found conserved among the tested

268 strains (**Figure 1, Table 2**). This fifth marker was non discriminating among the subset of
269 world-wide *Bathycoccus* strains.

270

271 *Accessory genes in Bathycoccus prasinus genome*

272 The large insertions found in the promoters of *yrdC* and *TOC1* were sequenced and analysed
273 in detail (**supplementary data 1A-B**).

274 In *yrdC* promoter, a gene encoding a protein of unknown function possessing ANK repeats
275 similar to the gene products of Bathy01g04610 (68% amino acid identity), Bathy01g04570
276 (67%) and Bathy11g02720 (57%) was inserted between an Evening Element-like (EEL) *cis*
277 element and the start of Bathy01g04300 in RCC5417, 1613, 685 and 4752. In order to gain
278 information on this additional gene, the Ocean Gene Atlas (OGA) website ([http://tara-](http://tara-oceans.mio.osupytheas.fr/ocean-gene-atlas/)
279 [oceans.mio.osupytheas.fr/ocean-gene-atlas/](http://tara-oceans.mio.osupytheas.fr/ocean-gene-atlas/)) (Villar et al., 2018, Vernet et al. 2022) was
280 interrogated with the additional protein and its three homologs. The only sequence retrieved
281 from OGA shared significant similarity with the 4 proteins but was not identical. So the
282 geographical distribution that we obtained is not the one corresponding to the accessory ANK
283 gene.

284 In *TOC1* promoter, the 2.2 kb insertion identified in RCC1613, RCC1615 and RCC4752
285 encodes a Methyltransferase-like protein (AdoMTase *METTL24* [IPR026913](#) IPR029063) of 320
286 aa with 41.7% amino acids identity to the predicted *Ostreococcus lucimarinus* CCE9901
287 protein (XP_001422352). Searches were performed at high stringency in OGA (Expect
288 threshold 1e-300) so that only the presence of the near-identical sequences was retrieved.
289 *TOC1* and AdoMTase sequences were not strictly co-occurring. At one station located near
290 Chile (**arrow Figure 2**), *TOC1* sequences were abundant but no AdoMTase was recorded
291 which suggests that in this particular area the *Bathycoccus* genomes are almost devoid of
292 AdoMTase. Surprisingly, it was possible to also find AdoMTase sequences not associated to

293 Bathycoccus TOC1 sequences indicating that this accessory gene can be found in other
294 unknown microorganisms suggesting possible horizontal gene transfer. Most AdoMTase hits
295 were found near the equator at temperature higher than 25°C. As a control, the co-occurrence
296 of TOC1 and CCA1 (Bathy06g4380) sequences was complete (**Supplemental Figure 1**).
297 Transcription of the gene encoding this AdoMTase was confirmed in the metaT database at
298 OGA (data not shown).

299 In conclusion, two large INDEL comprised additional genes and these should be considered
300 as structural rearrangements rather than simple INDEL. These accessory genes could
301 potentially be beneficial for adaptation.

302 ***Isolation of Bathycoccus during the 2018/2019 winter bloom***

303 Surface water was collected weekly from December 3rd to March 19th. During this period, the
304 sea temperature rose to 15.87°C in December and did not descent below 10.68°C in February
305 (**Figure 3A**). According to the 10-year study at the same location (SOLA Buoy in Banyuls
306 bay) for 2007-2015 ([Lambert et al. 2019](#)) and 2015-2017, this period can be considered as an
307 average climatic year in term of temperature ([Lambert et al. 2021](#)). The presence and
308 abundance of phytoplankton were determined by flow cytometry after filtration on 3 µm
309 (**Figure 3**). Whilst cyanobacteria were the most abundant at all time with a peak at the end of
310 February, picophytoplankton was the second most abundant category with a first peak in
311 December and a second in February (**Supplemental Figure 2**). At each sampling date,
312 collected seawater was also filtered through 1.2 µm pore-size and transferred to culture flasks.
313 After a period of acclimation of two weeks in supplemented sea water, cells were isolated by
314 plating on agarose. Light green-yellow coloured colonies were picked and sub-cultured. In
315 order to accelerate the identification of Bathycoccus among the isolated cells, amplifications
316 of a fragment of the *LOV-HK* (Bathy10g02360) gene were performed. These primers were
317 specific to the *Bathycoccus prasinos* genome and did not amplify the homologous gene in

318 *Ostreococcus* or *Micromonas* nor in any other species. The identity of these clones was
319 further confirmed by ribotyping (amplification of a 2kb ribosomal DNA fragment followed
320 by sequencing). In total, 55 *Bathycoccus* B1 genome isolates were recovered at nine sampling
321 dates ([Supplemental Table2](#)). Additional isolates producing ambiguous amplification of *LOV-*
322 *HK* were also ribotyped. Eleven were actually *Bathyococcus*, though not B1 type, and two
323 *Nanochloropsis* and four *Cylindrotheca* ([Supplemental Table2](#)).

324 ***Identification of dominant Bathycoccus Multi Loci Genotypes in Banyuls bay in 2018/2019***

325 The five diversity markers were used in a combination of PCR and sequencing in order to
326 distinguish the different isolates of *Bathycoccus* sampled during the 2018/2019 winter bloom.
327 For the *yrdC* promoter, the inserted gene encoding a protein with ANK repeats was not
328 detected in the Banyuls samples. In one isolate only (B1 February 25th), the *yrdC* promoter
329 was near identical to the one in RCC4222 (99% identity in 332 bp, [Supplemental data 1A](#)). In
330 54 other isolates, a fragment of 200 bp similar in size to that in RCC1868 was amplified and
331 sequenced (100% identity, [Supplemental data 1A](#)). The insertion present in the *TOC1*
332 promoter was more prevalent in the Banyuls isolates (91%) than in the world-wide strains
333 (43%) ([Table 2 and 3](#)). A high degree of similarity (98.6%) was observed over the entire
334 insertion whilst the core promoter of *TOC1* containing the essential Evening Element-Like
335 (EEL) *cis* element had a minimum of 71.6% nucleotide identity in 400 bp. A phylogenetic
336 tree was constructed with these sequences ([Supplemental data 1B](#)). The 2 kb inserted
337 sequence was not included in the study but its occurrence is indicated between brackets for
338 each isolate. Most of the Mediterranean isolates were found in the main clade which divided
339 further into two subclades Ia and Ib. Subclade Ia contained all the Mediterranean reference
340 type and RCCC685, while subclade Ib most of the Mediterranean 2kb type and RCC1615.
341 RCC1613 and RCC4752 from Naples lie in a separate clade II. RCC1868 and the Arctic
342 RCC5417 contained the most divergent sequences in clade III. As a consequence of the 2kb

343 insertion, the *TOCI* promoter activity is most likely not abolished since the crucial EEL *cis*
344 element is still present but the analysis of the core promoter sequences indicates that its
345 activity could differ between the clades. Thus the *TOCI* promoter could constitute a
346 functional marker as well as a diversity marker.

347 The gene encoding a flavodoxin-like protein was more diverse in size than were the intergenic
348 regions ([Supplemental data 1C, Table 2, 3](#)). The maximum size difference increases to 245
349 amino acids between B1, a February Banyuls isolate and the Arctic RCC5417 strain. The
350 function related to this sequence variation is unknown. It forms a coiled-coil structure of
351 several alpha-helices. Coiled-coil domains have been identified in enzymes where they
352 function as molecular spacers positioning catalytic activities. So the variable length of the
353 repeats could influence the activity of the flavodoxin-like protein.

354 The genome of most Banyuls isolates encoded a Zinc finger C2H2 protein with 6 ZF motifs
355 (Bathy15g02320, [Supplemental data 1D, Table 3](#)). Only three isolates from February
356 sampling were similar to RCC685 with an additional ZF motif.

357 Amplification of a fragment of 530 bp of TIM (TIMa) was observed in 65% (approximately
358 two thirds) of the isolates ([Table 3](#)). Based on ONT data for the A8 isolate, we designed an
359 additional primer in order to amplify a variant of TIM present in the remaining third of the
360 isolates, TIMb. The alignment of the two predicted variant proteins TIM4222 and TIMA8
361 showed that one third of the protein is well conserved while two thirds were more variable
362 ([Supplemental data 1E](#)). A phylogenetic tree further supported this dichotomy ([Figure 4](#)).
363 OGA MetaG database was interrogated with TIM4222 and TIMA8 and each retrieved a
364 single hit, respectively OGATIM4222 and OGATIMA8 confirming the existence of the 2
365 isoforms of TIM world-wide ([Figure 4B](#)). OGATIMA8 has a marked abundance for high
366 latitudes and cold temperatures in the Northern hemisphere while OGATIM4222 is more
367 widely distributed.

368 Based on the results described above, the Banyuls isolates were classified in eight MLG
369 (Table 3). MLG 1 and MLG 2 represent respectively 53% and 29% of the population. Since
370 the number of isolates from each sampling date was not identical (Supplemental Table 2), this
371 percentage may not be entirely representative. However the presence of MLG 1 and 2 in five
372 out of nine independent samplings rules out a bias due to experimental cloning during
373 a isolation, Figure 3). We can thus confidently state that these two MLG were dominant in
374 Banyuls bay during the 2018/2019 bloom. No isolate with a MLG identical to RCC4222 was
375 found.

376

377 *Determination of major allelic variants in environmental samples : a three year follow-up*

378 The identification of dominant MLG during the bloom 2018/2019 raises the question of their
379 yearly or occasional prevalence in Banyuls bay. Since isolating strains is highly time
380 consuming, an alternative approach was developed to estimate local diversity. Five litres of
381 seawater were sampled once a week and filtered between 3 and 0.8 μm . DNA extracted from
382 0.8 μm filters was used as template for PCR analysis using our set of diversity markers.
383 Samplings were performed during 3 successive blooms from 2018 to 2021 (Figure 3,
384 Supplemental Figure 2).

385 Variations in the yrdC and TOC1 promoters and TIM ORF sequences were analysed on these
386 environmental DNA samples. For markers of chromosome 3 and 15, despite the high
387 specificity of the primers on DNA of individual Bathycoccus (Table3), they could not be used
388 on complex environmental DNA samples due to the presence of high background for
389 flavodoxin sequences and to the marginal size difference for Zinc finger C2H2 variants.

390 The time of sampling is indicated as week of the month (e.g. Oct-01 = 1st week of October) to
391 facilitate the comparison between years. The complete dataset is presented in Supplemental
392 Figure 3 and Supplemental Table 3.

393 The initiation of the bloom was analysed during two consecutive years (Figure 5). In 2019,
394 the presence of Bathycoccus was detected in the third week of November with a clear
395 predominance of the 200 bp allele of yrdC promoter and the presence of both TIMa and
396 TIMb. In 2020, Bathycoccus was detected in October, was barely detected or absent in
397 November and reappeared in December, consistent with the recording the decrease of
398 abundance of picophytoplankton by flow cytometry (Supplemental Figure 2). In 2020, the
399 allelic ratios of 200/400 bp of the yrdC promoter were clearly different from those in 2019
400 and TIMb was not detected. We conclude that the populations at the onset of the bloom were
401 different in both timing and diversity.

402 The diversity of populations was also assessed during the bloom (Figure 5Figure 3). The
403 abundance of alleles of yrdC promoter and TIM were clearly different in November-
404 December compared to February.

405 In summary, the study of three successive blooms showed changes in the diversity of
406 Bathycoccus populations during a bloom, particularly at its onset and between years.

407

408 *Physiological characteristic of isolated Bathycoccus strains*

409 Since alleles abundance showed that November-December and February populations are
410 different and since temperature and light intensity are significantly different in December
411 (15.9°C, 9h15 light, maximum intensity 540 $\mu\text{E}/\text{m}^2/\text{s}$) and February (11.8°C, 10h30 light,
412 maximum intensity 830 $\mu\text{E}/\text{m}^2/\text{s}$), the physiological parameters of the “December “ and
413 “February” isolates were determined. C2, an isolate from January 28th was included in the
414 experiment. Cells were grown at 13°C or 16°C under December or February illumination. At
415 low temperature, all the “February” isolates grew better than the “December” cells
416 independently of the light regime (Figure 6). At 16°C, the fitness of “December” isolates B9
417 and G11 was significantly improved and reached the growth rate of the “February” cells.

418 February illumination conditions further reduced the fitness difference between “December”
419 and “February” isolates. Overall, the “February” isolates were more performing than the
420 December” isolates particularly at low temperature. Photosynthesis parameters were
421 determined by PhytoPAM. For most isolates, no significant differences in indicators of
422 photosynthesis parameters were observed with the exception of the B1 February isolate with
423 the unique MLG 7 ([Supplemental Figure 4](#)).

424 Together, the results showed a clear difference in the growth rate of the Bathycoccus isolated
425 in December and February mainly due their capacity of adaptation to low temperature.

426 ***Presence of additional Bathycoccus species in Banyuls***

427 Eleven isolates from December were characterised as Bathycoccus by their ribosomal 18S
428 sequences. However since specific primers for the LOV-HK gene and the TOC1 promoter did
429 not amplify a fragment using their DNA as template they were not B1 type. They could be of
430 B2 type. The presence of B2 Bathycoccus in Banyuls bay has been suggested by the TARA
431 metagenomic data analysis ([Vannier et al. 2016](#)). A closer examination of ITS2 sequences
432 showed that these 11 Bathycoccus were neither B1 nor B2 but a new type that we named B3
433 ([Figure 7A](#)). We included in the analysis a potential new Bathycoccus type identified among
434 uncultured seawater samples from Russian seas ([Belevich et al. 2021](#)) that we named B4 and
435 we showed that B3 is different from the 3 others.

436 In addition, primers were designed for the TOC1 promoter and the intein inserted into the
437 PRP8 gene in RCC716 B2 type genome and used them on Banyuls seawater. These 2 gene
438 portions (validated by sequencing, [Supplemental data 1F and 1G](#)) confirmed the presence of
439 Bathycoccus B2 type although none were isolated. Specific primers for B3 (TOC1 ORF) were
440 also used on environmental samples and taking together these results show that Bathycoccus
441 B1, B2 and B3 type were present from January to March 2019 in Banyuls bay ([Figure 7B](#)).
442 They relative abundance compared to the control DNA suggests that B2 and B3 were less

443 abundant than B1 in Banyuls. To provide additional evidence to classify Bathycoccus B3 type
444 as a new species, the cell ultrastructure were determined by electronic microscopy compared
445 to the one of B1 type. B3 cells showed the characteristic features of Bathycoccus with a single
446 chloroplast containing a single starch granule and scales at the surface. We named this new
447 species *Bathycoccus catiminus* (Figure 7C).

448 **Discussion (2340 words)**

449 *Contribution of ONT sequencing to the identification of Bathycoccus molecular markers*

450 Bathycoccus has a small genome of approximately 15 Mb distributed among 19
451 chromosomes and has only been found in an haploid phase (Moreau et al. 2012). This
452 organisation makes it suitable for Oxford Nanopore Technology Rapid barcoding libraries
453 and sequencing. On a single flow cell, it was possible to obtain sufficient coverage for the
454 genome of up to 3 strains. The main difficulty was to obtain good quality genomic DNA for
455 each strain, a criteria particularly important when pooling barcoded libraries. With the
456 exception of RCC1615, all ONT data were superior to 10 times the size of the Bathycoccus
457 genome (Table 1). When comparing ONT data from RCC4222 to the clonal RCC1105
458 reference, 19 INDEL were found. Two main reasons can be proposed. Firstly, RCC14222 is
459 not strictly identical to RCC1105. Secondly, ONT is particularly suitable to identify structural
460 variations previously undetected by conventional sequencing method (Michael et al. 2018,
461 Mantere et al. 2019). Therefore, most of the INDEL identified between RCC1105 and
462 RCC4222 genomes could result from the use of different sequencing techniques. To design
463 diversity markers, INDEL in intergenic regions (promoters) as well as ORF encoding repeat
464 amino acids sequences were selected. Most predictions were accurate and validated by PCR
465 and sequencing, except in two cases, where we could not design specific primers and the
466 marker status was unresolved (data not shown).

467 *Identification of Bathycoccus local diversity using INDEL markers*

468 The 55 Mediterranean B1 Bathycoccus isolates were genotyped using five INDEL markers
469 that were based on ONT sequencing of strains coming from contrasted geographic locations
470 between arctic and temperate regions. The percentage of the presence of a marker type was
471 quite different between the world-wide strains and the Banyuls strains ([Table 2 and 3](#)). For
472 example, the insertion of a gene encoding ANK repeats was found in four out of seven world
473 strains but was absent from Banyuls strains, while the insertion of the AdoMTase into the
474 TOC1 promoter was much more prevalent in Banyuls strains. In general, the genome of
475 Banyuls Bathycoccus isolates possesses allelic variants common to most of them (65-98%,
476 [Table 3](#)) representing the dominant MLG 1 and 2. Remarkably, these three dominant
477 INDEL/rearrangements (200 bp yrdC, 2.2 Kb TOC1, 1.2 Kb Flavodoxin) were not found in
478 the reference genome RCC4222 that was isolated in the Banyuls bay in 2006. In addition, no
479 2018-2019 isolates share the same five marker types with either the Banyuls reference nor the
480 RCC4752 Napoli genome that was isolated in 1986 ([Table 3](#)). Thus it is clear that RCC4222
481 isolated in Banyuls bay in 2006 was certainly not abundant and probably not present during
482 the bloom 2018/2019. Overall we did not observe any obvious consistent pattern of
483 occurrence between specific markers and the geographic origin of the world-wide strains
484 ([Table 2 and 3](#)).

485 The determination of eight MLG in Bathycoccus is probably an underestimation. For example
486 in diatoms, where more than 600 individuals have been genotyped using microsatellites, it
487 was estimated that the blooming population was comprised of at least 2400 different
488 genotypes ([Rynearson and Armbrust 2005](#)). However the dominance of two MLG among
489 Bathycoccus isolates is probably accurate, despite being based on a small number.

490 The existence of major MLG highlights an apparent paradox : how can blooms be diverse,
491 given that the best genotype should prevail? Blooms are predicted to quickly become
492 dominated by a few particularly well-adapted genotypes ([De Meester, 1996](#)). Nevertheless,

493 most studies describing genetic diversity of blooming phytoplankton populations report high
494 intraspecific variation (Rynearson and Armbrust, 2005; Alpermann et al., 2009 ; Lebret et al.,
495 2012 ; Dia et al., 2014). Indeed, our results revealed such diversity by the detection of six
496 minor MLG beside the two major ones. Remarkably, the different fitness observed between
497 December and February 2018/2019 isolates correlates with differences in allelic frequencies
498 at onset of a bloom and during the course of a bloom as determined on seawater samples,
499 suggesting that best seasonal MLG may become dominant at specific times of the year.
500 Similarly, temporal succession of two genetically distinct sub-populations was observed
501 during the bloom of the haploid *Alexandrium dinoflagellate* in Gulf of Maine (Erdner et al.,
502 2011).

503 Finally, in addition to eight *Bathycoccus prasinus* MLG (B1), we identified two other
504 *Bathycoccus* species, including the previously described species *Bathycoccus calidus* (B2)
505 and a yet not described *Bathycoccus* B3 species that we name *B. catiminus*. Our results
506 clearly demonstrate that under a single *Bathycoccus* 18S ribotype are hidden at least three
507 distinct species. This emphasises the necessity of isolating new *Bathycoccus* to design
508 interspecific markers that could be used on environmental samples and metagenomic datasets
509 in order to understand the dynamics of *Bathycoccus* blooms and the adaptation of this
510 cosmopolitan genus in the world ocean.

511

512 ***Structural variants as intraspecies markers to follow intra-specific diversity in***
513 ***environmental samples***

514 Historically, the intraspecies markers corresponded to small nucleotide repeats
515 (microsatellites) or chloroplastic or mitochondrial genes and a few nuclear genes that were
516 applied to several hundreds of isolated individuals. The development of Restriction-site-
517 Associated DNA sequencing (RADseq) techniques has allowed the discovery and genotyping

518 of thousands of genetic markers for any given species at relatively low-cost ([Andrews et al.](#)
519 [2016](#)). Some of these approaches have been used to analyse the diversity of populations
520 during algal blooms ([Regenfors et al. 2017](#)). The recent dramatic increase of the number of
521 sequenced genomes led to large-scale diversity studies with large sets of nuclear genes or
522 whole genome comparisons. Most of these approaches required the isolation of a large
523 number of individuals. As a consequence, intraspecies diversity has been poorly documented
524 in the past in marine phytoplankton. Novel, rapid and cheap sequencing technologies have
525 given access to Mamiellales diversity by the sequencing of the genomes of *Ostreococcus*
526 isolates ([Blanc-Mathieu et al. 2017](#)) or by metagenomic approaches ([Leconte et al. 2020](#), [Da](#)
527 [Silva et al. 2022](#); [Richter et al. 2022](#)) or metatranscriptomic approaches ([Simmons et al.](#)
528 [2016](#)).

529 We aimed to develop a rapid and cost effective alternative which did not rely on isolated
530 individuals since it is very challenging and time consuming to isolate marine microalgae from
531 complex microbial communities. Compared to short read sequencings, the recent ONT and
532 PACBIO sequencing technology provided information on structural variants, in particular on
533 relatively large INDEL and on repeated/low complexity sequences, with some of which
534 previously overlooked ([Wellenreuther et al. 2019](#)). This knowledge was particularly useful to
535 develop a novel type of marker for assessing intraspecies diversity that will rely only on PCR
536 amplification of variable size fragment without the need of sequencing. Furthermore, with
537 INDEL based on ONT we are reaching a higher level of population structure compared to
538 microsatellite or SNP markers. Structural variants are expected to be less neutral and more
539 stable than microsatellites ([Mérot et al. 2020](#)). Microsatellites can change in clonal strains of
540 *P. multistriata* in the laboratory over several months ([Ruggiero et al. 2018](#)), while our
541 structural markers are still identical in the reference genome published in 2012 and its clonal
542 strain RCC4222 sequenced in 2018. Thus INDEL markers can identify large subpopulations

543 rather than small groups of individuals. Our studies on three successive blooms in Banyuls
544 showed that the ONT designed markers are capable of determining the dominant allelic
545 variants and their perennial occurrence. Similarly these INDEL markers could be used as
546 query on metagenomic databases for a wider and large analysis of *Bathycoccus* populations.
547
548 Variations in allele frequencies were observed for three consecutive years, raising the
549 question of the nature of the highly reproducible yearly re-occurrence of *Bathycoccus* in the
550 bay of Banyuls. Seasonal blooms may result either from re-activation of “dormant/survivor”
551 cells from the water column (whose genetic fingerprint will determine the genetic profile of
552 the next bloom) or by yearly *de novo* fertilisation by cells carried by the north Mediterranean
553 current along the gulf of Lion. At the first glance, our preliminary results are in favour of the
554 introduction of a new population rather than “resuscitation” of cells of the previous bloom
555 since allelic frequencies are distinct between the end of a bloom o the onset of the next
556 (Figure 5). By monitored the temporal population structures of the dinoflagellate *Alexandrium*
557 *minutum* in two estuaries in France, [Dia et al. \(2014\)](#) showed that interannual genetic
558 differentiation was greater than intra-bloom differentiation. Alternation of
559 genotypes/populations has also been observed with diatoms in the dominance of one of the
560 two sympatric populations of *Pseudonitzschia multistriata* which could be due either to
561 environmental factors favouring one population over the other or intrinsic factors coupled to
562 the obligate sexual life cycle of *P. multistriata* ([D’Alelio et al. 2010](#)). Thus the observed
563 differences in alleles frequencies could equally be the result of new inoculum from currents
564 or of sexual reproduction. Even though sexual reproduction has not been demonstrated in
565 *Bathycoccus*, there is genomic evidence that it may occur ([Benites et al. 2021](#)). Sexual
566 recombination generates new combinations of alleles, whereas clonality favours the spread of
567 the fittest genotype through the entire population ([Dia et al. 2014](#)). [Erdner et al. \(2011\)](#)

568 propose for *A. fundyense* that mitosis is the primary mode of multiplication during blooms
569 whereas mating is triggered presumably in response to unfavourable conditions at the end of
570 blooms, with vegetative cells not overwintering in the water column. In Banyuls bay, the
571 abundance during the bloom is followed by severe bottlenecks in which *Bathycoccus* are
572 hardly detected in the water column ([Lambert et al. 2019](#)).

573 Knowing that (1) *Bathycoccus* blooms are followed by severe bottlenecks between one bloom
574 and the next, (2) allelic frequencies were not similar at the end of one bloom and at the onset
575 of the next and (3) structural markers are very stable in mitotic dividing cells, the hypothesis
576 of rare vegetative cells remaining in the water column between the blooms is unlikely except
577 if those remaining cells were produced by sexual reproduction. The other hypothesis of new
578 strains brought by current is equally probable.

579

580 ***Structural variants versus functional variants***

581 Our principal interest was to identify markers of intraspecies diversity in order to follow the
582 dynamics of *Bathycoccus* population during annual blooms in the bay of Banyuls. However
583 structural variants are probably not neutral markers unlike microsatellites. Most of the
584 selected markers could also represent functionally significant variants such as an additional
585 gene or a modified promoter activity or protein function, that could correspond to an
586 adaptation to contrasted intra- and interannual variations in environmental parameters in the
587 Banyuls Bay ([Lambert et al., 2021](#)).

588

589 In only five worldwide INDEL, we discovered two additional genes in the genome of
590 *Bathycoccus prasinus* and a particular protein structure. The additional ANK repeat encoding
591 gene in chromosome 1 has probably arisen by gene duplication or gene loss since it belongs
592 to a multigenic family. The origin of the AdoMTase could be the result of Horizontal Gene

593 Transfer. The Flavodoxin-like protein has an organisation specific to Bathycoccus with a
594 coiled-coil domain of variable size with similarity to Eukaryotes parasites and toxic bacteria
595 proteins and a flavodoxin domain found in the 7 other Bathycoccus flavodoxin-like proteins.
596 Bathycoccus culture strains do not possess a flavodoxin per se while it was found in
597 uncultured Bathycoccus (Pierella Karlusich et al. 2015). This peculiar flavodoxin-like protein
598 could represent a case of neofunctionalisation in Bathycoccus. The core promoter of the
599 central circadian clock *TOC1* gene has a conserved evening element like box (EEL box) that
600 has been experimentally demonstrated as essential in the central oscillator of *Ostreococcus*
601 *tauri* (Corellou et al. 2009). Although the EEL box is found in all the accessions sequenced,
602 the distance between the *cis* element and the initiation codon is variable. In addition, the
603 phylogenetic tree of the core promoter sequences clearly discriminated the Arctic RCC5417
604 and RCC1868 and to a lesser extent, RCC1613 and the second Mediterranean strain,
605 RCC4752 (Suppl. data 1B). An insertion of the AdoMTase was found about 100 bp upstream
606 the EEL box. This insertion could potentially modify the promoter activity and ultimately the
607 expression pattern of *TOC1*. Such a natural variation of promoter length modulates the
608 photoperiodic response of FLOWERING LOCUS T by differentially spacing two
609 interdependent regulatory regions (Liu et al. 2014). Although the presence of the AdoMTase
610 was not correlated with the latitude or the temperature in the Ocean Gene Atlas (Figure 2), it
611 could still be associated with a seasonal niche. Less information is available for the promoter
612 and function of the *yrDC* gene. The rearrangements are more drastic, specially with the
613 displacement of the EEL box by insertion or deletion, and could lead to the inactivation of the
614 promoter. The most striking feature concerns the TIM protein where only one third of the
615 protein is conserved between TIMa and TIMb. Due to its position in the BOC of chromosome
616 14 putatively involved in mating, this raises the question of the mating types of cells with
617 genome containing TIMa or a genome with TIMb.

618 Altogether, this analysis suggests that our allelic markers may be more than diversity markers,
619 being potentially involved in adaptation to changing environmental conditions.

620 **Conclusions and perspectives**

621 In this paper we analysed the populations of *Bathycoccus* blooming in the Banyuls
622 bay. Based on structural variants, the isolates were categorised into eight MLG with two
623 dominant classes. The survey of *Bathycoccus* diversity in environmental samples during three
624 successive blooms confirms the yearly presence of dominant allelic variants that were
625 different within and between years. This pioneer study on *Bathycoccus* diversity in the bay of
626 Banyuls now paves the way to an in depth analysis of multiple markers present in more than a
627 decade of bimonthly sampled metagenomic data at a discrete location ([Lambert et al. 2019](#);
628 [Lambert et al. 2021](#)). The sequencing of the whole genomes of the different MLG, together
629 with the assessment of their physiological performances will bring additional information
630 contributing to the local diversity of *Bathycoccus* and provide insight their seasonal pattern of
631 abundance. In addition, these diversity markers represent an essential tool for grasping the
632 maximum diversity of newly isolated *Bathycoccus* world-wide and identify putative
633 molecular mechanisms involved in adaptation to environmental niches of this cosmopolitan
634 genus.

635 **Acknowledgments**

636 We are grateful to the captain and the crew of the RV 'Nereis II' for their help in acquiring the
637 samples. Additional ONT were performed with the help of Christel Llauro and Marie Mirouze
638 LGDP. The authors acknowledge the ISO 9001 certified IRD itrop HPC (member of the
639 South Green Platform) at IRD Montpellier for providing HPC resources that have contributed
640 to the research results reported within this paper (URL: <https://bioinfo.ird.fr/> -
641 <http://www.southgreen.fr>). The work was financed by a internal LOMIC Microprojet and the
642 ANR Climaclock 2020-2024. We are thankful to Marie-Line Escande and the platform

643 PioPIC at the Banyuls Oceanographic Observatory for electron microscopy service. We thank
644 Thomas Roscoe for critical reading the manuscript.

645

646 **References (1875 words)**

647 [Alonge](#) M, Soyk S, Ramakrishnan S, Wang X, Goodwin S, Sedlazeck FJ, Lippman ZB,
648 Schatz MC. (2019) RaGOO: fast and accurate reference-guided scaffolding of draft genomes.
649 *Genome Biol.* 20(1):224. doi: 10.1186/s13059-019-1829-6.

650 [Alpermann](#) TJ, Beszteri B, John U, Tillmann U, Cembella AD. (2009) Implications of life-
651 history transitions on the population genetic structure of the toxigenic marine dinoflagellate
652 *Alexandrium tamarense*. *Molecular Ecology*, 18(10):2122-33. doi: 10.1111/j.1365-
653 294X.2009.04165.x.

654 [Andrews](#) KR, Good JM, Miller MR, Luikart G, Hohenlohe PA. (2016) Harnessing the power
655 of RADseq for ecological and evolutionary genomics. *Nature Reviews Genetics*, 17(2):81-92.
656 doi: 10.1038/nrg.2015.28.

657 [Bachy](#) C, Yung CCM, Needham DM, Gazitúa MC, Roux S, Limardo AJ, Choi CJ, Jorgens
658 DM, Sullivan MB, Worden AZ. (2021) Viruses infecting a warm water picoeukaryote shed
659 light on spatial co-occurrence dynamics of marine viruses and their hosts. *The ISME Journal*,
660 doi: 10.1038/s41396-021-00989-9.

661 [Belevich](#) TA, Milyutina IA, Abyzova GA, Troitsky AV. (2021) The pico-sized
662 Mamiellophyceae and a novel Bathycoccus clade from the summer plankton of Russian
663 Arctic Seas and adjacent waters. *FEMS Microbiology Ecology*, 97(2):fiae251. doi:
664 10.1093/femsec/fiae251.

665 [Benites](#) LF, Bucchini F, Sanchez-Brosseau S, Grimsley N, Vandepoele K, Piganeau G. (2021)
666 Evolutionary Genomics of Sex-Related Chromosomes at the Base of the Green Lineage.
667 *Genome Biology Evolution*, 13(10):evab216. doi: 10.1093/gbe/evab216.

- 668 [Blanc-Mathieu](#) R, Krasovec M, Hebrard M, Yau S, Desgranges E, Martin J, Schackwitz W,
669 Kuo A, Salin G, Donnadiou C, Desdevises Y, Sanchez-Ferandin S, Moreau H, Rivals E,
670 Grigoriev IV, Grimsley N, Eyre-Walker A, Piganeau G. (2017) Population genomics of
671 picophytoplankton unveils novel chromosome hypervariability. *Science Advances*,
672 3(7):e1700239. doi: 10.1126/sciadv.1700239.
- 673 [Chrétionot-Dinet](#) MJ, Courties C, Vaquer A, Neveux J, laustre H, autrier J and Machado MC
674 1995. A new marine picoeucaryote: *Ostreococcus tauri* gen. et sp. nov. (Chlorophyta,
675 Prasinophyceae). *Phycologia*, 34(4): 285–292.
- 676 [Corellou](#) F, Schwartz C, Motta JP, Djouani-Tahri el B, Sanchez F, Bouget FY. (2009) Clocks
677 in the green lineage: comparative functional analysis of the circadian architecture of the
678 picoeukaryote *ostreococcus*. *The Plant Cell*, 21(11):3436-49. doi: 10.1105/tpc.109.068825.
- 679 [D’Alelio D](#), Ribera d’Alcala M, Dubroca L, Sarno D, Zingone A, Montresor M (2010) The
680 time for sex: A biennial life cycle in a marine planktonic diatom *Limnol.ogy Oceanography*,
681 55(1) 106–114.
- 682 [Da Silva O](#), Ayata SD, Ser-Giacomi E, Leconte J, Pelletier E, Fauvelot C, Madoui MA, Guidi
683 L, Lombard F, Bittner L (2022) Genomic differentiation of three pico-phytoplankton species
684 in the Mediterranean Sea. *Environmental Microbiology*, Aug 16. doi: 10.1111/1462-
685 2920.16171.
- 686 [Debladis](#) E, Llauro C, Carpentier MC, Mirouze M, Panaud O. (2017) Detection of active
687 transposable elements in *Arabidopsis thaliana* using Oxford Nanopore Sequencing
688 technology. *BMC Genomics*, 18(1):537. doi: 10.1186/s12864-017-3753-z.
- 689 [De Coster](#) W, D’Hert S, Schultz DT, Cruts M, Van Broeckhoven C. (2018) NanoPack:
690 visualizing and processing long-read sequencing data. *Bioinformatics* 34(15):2666-2669. doi:
691 10.1093/bioinformatics/bty149.

- 692 [De Meester L.](#) (1996) Evolutionary potential and local genetic differentiation in a
693 phenotypically plastic trait of a cyclical ârthenogen *Daphnia Magna*. *Evolution*, 50(3):1293-
694 1298. doi: 10.1111/j.1558-5646.1996.tb02369.x.
- 695 [Des Roches S](#), Post DM, Turley NE, Bailey JK, Hendry AP, Kinnison MT, Schweitzer JA,
696 Palkovacs EP (2018) The ecological importance of intraspecific variation. *Nature Ecology*
697 *Evolution*, 2(1):57-64. doi: 10.1038/s41559-017-0402-5.
- 698 [Dia A](#), Guillou L, Mauger S, Bigeard E, Marie D, Valero M, Destombe C. (2014)
699 Spatiotemporal changes in the genetic diversity of harmful algal blooms caused by the toxic
700 dinoflagellate *Alexandrium minutum*. *Molecular Ecology*, 23(3):549-60. doi:
701 10.1111/mec.12617.
- 702 [Erdner DL](#), Richlen M, McCauley LA, Anderson DM. (2011) Diversity and dynamics of a
703 widespread bloom of the toxic dinoflagellate *Alexandrium fundyense* *PLoS One*,
704 6(7):e22965. doi: 10.1371/journal.pone.0022965.
- 705 [Gallagher JC](#) (1980) Population genetics of *Skeletonema costatum* (Bacillariophyceae) in
706 Narragansett bay. *Journal of Phycology*, 16, 464-474 doi.org/10.1111/j.1529-
707 8817.1980.tb03061.x
- 708 [Galtier N](#), Nabholz B, Glémin S, Hurst GD. (2009) Mitochondrial DNA as a marker of
709 molecular diversity: a reappraisal. *Molecular Ecology*, 18(22):4541-50. doi: 10.1111/j.1365-
710 294X.2009.04380.x.
- 711 [Godhe A](#), Rynearson T. (2017) The role of intraspecific variation in the ecological and
712 evolutionary success of diatoms in changing environments. *Philosophical Transaction of the*
713 *Royal Society London B Biological Sciences*, 5;372(1728):20160399. doi:
714 10.1098/rstb.2016.0399.
- 715 [Guyon JB](#), Vergé V, Schatt P, Lozano JC, Liennard M, Bouget FY. (2018) Comparative
716 Analysis of Culture Conditions for the Optimization of Carotenoid Production in Several

- 717 Strains of the Picoeukaryote *Ostreococcus*. *Marine Drugs*, 16(3):76. doi:
718 10.3390/md16030076.
- 719 [Joli N](#), Monier A, Logares R, Lovejoy C. (2017) Seasonal patterns in Arctic prasinophytes
720 and inferred ecology of *Bathycoccus* unveiled in an Arctic winter metagenome. *The ISME*
721 *Journal*, 11(6):1372-1385. doi: 10.1038/ismej.2017.7.
- 722 [Kashtan N](#), Roggensack SE, Rodrigue S, Thompson JW, Biller SJ, Coe A, Ding H, Marttinen
723 P, Malmstrom RR, Stocker R, Follows MJ, Stepanauskas R, Chisholm SW. (2014) Single-cell
724 genomics reveals hundreds of coexisting subpopulations in wild *Prochlorococcus*. *Science*,
725 344(6182):416-20. doi: 10.1126/science.1248575.
- 726 [Kolmogorov M](#), Yuan J, Lin Y, Pevzner PA. (2019) Assembly of long, error-prone reads
727 using repeat graphs. *Nat Biotechnol.* 37(5):540-546. doi: 10.1038/s41587-019-0072-8.
- 728 [Lambert S](#), Tragin M, Lozano JC, Ghiglione JF, Vaultot D, Bouget FY, Galand PE. (2019)
729 Rhythmicity of coastal marine picoeukaryotes, bacteria and archaea despite irregular
730 environmental perturbations. *The ISME Journal*, 13(2):388-401. doi: 10.1038/s41396-018-
731 0281-z.
- 732 [Lambert S](#), Lozano JC, Bouget FY, Galand PE. (2021) Seasonal marine microorganisms
733 change neighbours under contrasting environmental conditions. *Environmental Microbiology*,
734 23(5):2592-2604. doi: 10.1111/1462-2920.15482. Epub 2021
- 735 [Lebret K](#), Kritzberg ES, Figueroa R, Rengefors K. *Environ Microbiol.* (2012) Genetic
736 diversity within and genetic differentiation between blooms of a microalgal species.
737 *Environmental Microbiology*, 14(9):2395-404. doi: 10.1111/j.1462-2920.2012.02769.x.
- 738 [Leconte J](#), Benites LF, Vannier T, Wincker P, Piganeau G, Jaillon O. (2020) Genome
739 Resolved Biogeography of Mamiellales. *Genes (Basel)*, 11(1):66. doi:
740 10.3390/genes11010066.

- 741 [Li H.](#) (2021) New strategies to improve minimap2 alignment accuracy. *Bioinformatics*
742 37(23):4572-4. doi: 10.1093/bioinformatics/btab705.
- 743 [Li WK,](#) Rao DV, Harrison WG, Smith JC, Cullen JJ, Irwin B, Platt T. (1983) Autotrophic
744 picoplankton in the tropical ocean. *Science*, **219**: 292-5.
- 745 [Limardo AJ,](#) Sudek S, Choi CJ, Poirier C, Rii YM, Blum M, Roth R, Goodenough U, Church
746 MJ, Worden AZ. (2017) Quantitative biogeography of picoprasinophytes establishes ecotype
747 distributions and significant contributions to marine phytoplankton. *Environmental*
748 *Microbiology*, 19(8):3219-3234. doi: 10.1111/1462-2920.13812.
- 749 [Liu L,](#) Adrian J, Pankin A, Hu J, Dong X, von Korff M, Turck F. (2014) Induced and natural
750 variation of promoter length modulates the photoperiodic response of FLOWERING LOCUS
751 T. *Nature Communications*, 5:4558. doi: 10.1038/ncomms5558.
- 752 [Mantere T,](#) Kersten S, Hoischen A. Long-Read Sequencing Emerging in Medical Genetics.
753 (2019) *Frontiers in Genetics*, 10:426. doi: 10.3389/fgene.2019.00426.
- 754 [Mérot C,](#) Oomen RA, Tigano A, Wellenreuther M. (2020) A Roadmap for Understanding the
755 Evolutionary Significance of Structural Genomic Variation. *Trends Ecol Evol.* 35(7):561-
756 572. doi: 10.1016/j.tree.2020.03.002.
- 757 [Michael TP,](#) Jupe F, Bemm F, Motley ST, Sandoval JP, Lanz C, Loudet O, Weigel D, Ecker
758 JR. (2018) High contiguity *Arabidopsis thaliana* genome assembly with a single nanopore
759 flow cell. *Nature Communications*, 9(1):541. doi: 10.1038/s41467-018-03016-2.
- 760 [Mikheenko A,](#) Prjibelski A, Saveliev V, Antipov D, Gurevich A. (2018) Versatile genome
761 assembly evaluation with QUASt-LG. *Bioinformatics* 34(13):i142-i150. doi:
762 10.1093/bioinformatics/bty266.

- 763 [Monier A](#), Sudek S, Fast NM, Worden AZ. (2013) Gene invasion in distant eukaryotic
764 lineages: discovery of mutually exclusive genetic elements reveals marine biodiversity. *The*
765 *ISME Journal*, 7(9):1764-74. doi: 10.1038/ismej.2013.70.
- 766 [Moreau H](#), Verhelst B, Couloux A, Derelle E, Rombauts S, Grimsley N, Van Bel M, Poulain
767 J, Katinka M, Hohmann-Marriott MF, Piganeau G, Rouzé P, Da Silva C, Wincker P, Van de
768 Peer Y, Vandepoele K. (2012) Gene functionalities and genome structure in Bathycoccus
769 prasinos reflect cellular specializations at the base of the green lineage. *Genome Biology*,
770 13(8):R74. doi: 10.1186/gb-2012-13-8-r74.
- 771 [Pierella Karlusich JJ](#), Ceccoli RD, Graña M, Romero H, Carrillo N. (2015) Environmental
772 selection pressures related to iron utilization are involved in the loss of the flavodoxin gene
773 from the plant genome. *Genome Biology and Evolution*, 7(3):750-67. doi:
774 10.1093/gbe/evv031.
- 775 [Raffard A](#), Santoul F, Cucherousset J, Blanchet S. (2019) The community and ecosystem
776 consequences of intraspecific diversity: a meta-analysis. *Biological Reviews of the Cambridge*
777 *Philosophical Society*, 94(2):648-661. doi: 10.1111/brv.12472.
- 778 [Read BA](#), Kegel J, Klute MJ, Kuo A, Lefebvre SC, Maumus F, Mayer C, Miller J, Monier A,
779 Salamov A, Young J, Aguilar M, Claverie JM, Frickenhaus S, Gonzalez K, Herman EK, Lin
780 YC, Napier J, Ogata H, Sarno AF, Shmutz J, Schroeder D, de Vargas C, Verret F, von
781 Dassow P, Valentin K, Van de Peer Y, Wheeler G; Emiliania huxleyi Annotation Consortium,
782 Dacks JB, Delwiche CF, Dyhrman ST, Glöckner G, John U, Richards T, Worden AZ, Zhang
783 X, Grigoriev IV. Pan genome of the phytoplankton Emiliania underpins its global
784 distribution. (2013) *Nature*, 499(7457):209-13. doi: 10.1038/nature12221.
- 785 [Rengefors, K.](#), Kremp, A., Reusch, T.B.H. and Wood A. M. (2017) Genetic diversity and
786 evolution in eukaryotic phytoplankton: revelations from population genetic studies. *Journal of*
787 *Plankton Research*, (2017) 39(2): 165– 179.

788 [Richter](#) DJ, Watteaux R, Vannier T, Leconte J, Frémont P, Reygondeau G, Maillet N, Henry
789 N, Benoit G, Da Silva O, Delmont TO, Fernández-Guerra A, Suweis S, Narci R, Berney C,
790 Eveillard D, Gavory F, Guidi L, Labadie K, Mahieu E, Poulain J, Romac S, Roux S, Dimier
791 C, Kandels S, Picheral M, Searson S; Tara Oceans Coordinators, Pesant S, Aury JM, Brum
792 JR, Lemaitre C, Pelletier E, Bork P, Sunagawa S, Lombard F, Karp-Boss L, Bowler C,
793 Sullivan MB, Karsenti E, Mariadassou M, Probert I, Peterlongo P, Wincker P, de Vargas C,
794 Ribera d'Alcalà M, Iudicone D, Jaillon O. (2022) Genomic evidence for global ocean
795 plankton biogeography shaped by large-scale current systems. *Elife*, 11:e78129. doi:
796 10.7554/eLife.78129.

797 [Ruggiero](#) MV, D'Alelio D, Ferrante MI, Santoro M, Vitale L, Procaccini G, Montresor M.
798 (2018) Clonal expansion behind a marine diatom bloom. *The ISME Journal*, 2018
799 Feb;12(2):463-472. doi: 10.1038/ismej.2017.181.

800 [Rynearson](#) TA, Armbrust EV. (2005) Maintenance of clonal diversity during a spring bloom
801 of the centric diatom *Ditylum brightwellii*. *Molecular Ecology*, 14(6):1631-40. doi:
802 10.1111/j.1365-294X.2005.02526.x.

803 [Sehgal](#) A, Rothenfluh-Hilfiker A, Hunter-Ensor M, Chen Y, Myers MP, Young MW (1995).
804 "Rhythmic expression of timeless: a basis for promoting circadian cycles in period gene
805 autoregulation". *Science*, 270 (5237): 808–10. doi:10.1126/science.270.5237.808.

806 [Simmons](#) MP, Sudek S, Monier A, Limardo AJ, Jimenez V, Perle CR, Elrod VA, Pennington
807 JT, Worden AZ. (2016) Abundance and Biogeography of Picoprasinophyte Ecotypes and
808 Other Phytoplankton in the Eastern North Pacific Ocean. *Applied Environmental*
809 *Microbiology*, 82(6):1693-1705. doi: 10.1128/AEM.02730-15.

810 [Srivastava](#) S, Avvaru AK, Sowpati DT, Mishra RK. (2019) Patterns of microsatellite
811 distribution across eukaryotic genomes. *BMC Genomics*, 20(1):153. doi: 10.1186/s12864-
812 019-5516-5.

- 813 [Teplova](#) M, Tereshko V, Sanishvili R, Joachimiak A, Bushueva T, Anderson WF, Egli M.
814 (2000) The structure of the yrdC gene product from Escherichia coli reveals a new fold and
815 suggests a role in RNA binding. *Protein Science*, 9(12):2557-66. doi: 10.1110/ps.9.12.2557.
- 816 [Tesson](#) SV, Borra M, Kooistra WH, Procaccini G. (2011) Microsatellite primers in the
817 planktonic diatom Pseudo-nitzschia multistriata (Bacillariophyceae). *American Journal of*
818 *Botany*, 98(2):e33-5.
- 819 [Tesson](#) SV, Montresor M, Procaccini G, Kooistra WH. (2014) Temporal changes in
820 population structure of a marine planktonic diatom. *PLoS One*, 9(12):e114984. doi:
821 10.1371/journal.pone.0114984.
- 822 [Tragin](#) M, Zingone A, Vaultot D (2018) Comparison of coastal phytoplankton composition
823 estimated from the V4 and V9 regions of the 18S rRNA gene with a focus on photosynthetic
824 groups and especially Chlorophyta. *Environmental Microbiology*, 20(2):506-520.
- 825 [Van den Wyngaert](#) S, Möst M, Freimann R, Ibelings BW, Spaak P. (2015) Hidden diversity
826 in the freshwater planktonic diatom Asterionella formosa. *Molecular Ecology*, 24(12):2955-
827 72. doi: 10.1111/mec.13218.
- 828 [Vannier](#) T, Leconte J, Seeleuthner Y, Mondy S, Pelletier E, Aury JM, de Vargas C, Sieracki
829 M, Iudicone D, Vaultot D, Wincker P, Jaillon O. Survey of the green picoalga Bathycoccus
830 genomes in the global ocean. (2016) *Scientific Reports*, 6:37900. doi: 10.1038/srep37900.
- 831 [Vaser](#) R, Sović I, Nagarajan N, Šikić M. (2017) Fast and accurate de novo genome assembly
832 from long uncorrected reads. *Genome Res.* 27(5):737-746. doi: 10.1101/gr.214270.116.
- 833 [Verette](#) C, Lecubin J, Sánchez P; Tara Oceans Coordinators, Sunagawa S, Delmont TO,
834 Acinas SG, Pelletier E, Hingamp P, Lescot M. (2022) The Ocean Gene Atlas v2.0: online
835 exploration of the biogeography and phylogeny of plankton genes. *Nucleic Acids Research*,
836 50(W1):W516-26. doi: 10.1093/nar/gkac420

837 .Villar E, T. Vannier, C. Vernet, M. Lescot, M. Cuenca, A. Alexandre, P. Bachelerie, T.
838 Rosnet, E. Pelletier, S. Sunagawa, P. Hingamp. (2018) The Ocean Gene Atlas: exploring the
839 biogeography of plankton genes online. *Nucleic Acids Research*, doi: 10.1093/nar/gky376.
840 Violle C, Enquist BJ, McGill BJ, Jiang L, Albert CH, Hulshof C, Jung V, Messier J. (2012)
841 The return of the variance: intraspecific variability in community ecology. *Trends in Ecology*
842 *and Evolution*, 27(4):244-52. doi: 10.1016/j.tree.2011.11.014.
843 Wellenreuther M, Mérot C, Berdan E, Bernatchez L (2019) Going beyond SNPs: The role of
844 structural genomic variants in adaptive evolution and species diversification. *Molecular*
845 *Ecology*, 28(6):1203-1209. doi: 10.1111/mec.15066.
846 Wheeler GL, Dorman HE, Buchanan A, Challagundla L, Wallace LE. (2014) A review of the
847 prevalence, utility, and caveats of using chloroplast simple sequence repeats for studies of
848 plant biology. *Applications in Plant Sciences*, 2(12):apps.1400059. doi:
849 10.3732/apps.1400059.

850 **Data accessibility**

851 Strains isolated in Banyuls have been sent to Roscoff Collection Centre and will be publicly
852 available after curation by the Centre. For whole genome sequences, basecalled reads and
853 RaGOO output for the 7 RCC strains used in this study are available at [????](#)

854 **Author contribution**

855 MD, FYB and FS conceived the work and acquired funding. MD extracted high molecular
856 weighty genomic DNA. ONT sequencing was performed by CM and MD and sequence
857 analysis by LD and FS. Diversity markers were designed and validated by MD. PS analysed
858 seawater samplings by flow cytometry. MD and VV isolated Banyuls strains during the
859 winter bloom, genotyped by MD and JCL. MD determined diversity of seawater. MD and
860 FYB wrote the article and all authors participated in critical revisions and approved the final
861 version for submission.

- 862 **Figure 1.** Diversity markers among world wide accessions
- 863 **Figure 2.** Geographical distribution of TOC1 and AdoMTase proteins
- 864 **Figure 3.** Abundance of phytoplankton during three successive blooms
- 865 **Figure 4.** Distribution and abundance of TIM variant proteins in MetaG database
- 866 **Figure 5.** Diversity markers in seawater
- 867 **Figure 6.** Growth of Mediterranean Bathycoccus isolates
- 868 **Figure 7.** Presence of two additional Bathycoccus species in Banyuls bay
- 869 **Table 1.** Number and sizes of INDEL
- 870 **Table 2.** Distribution of diversity markers in world-wide strains
- 871 **Table 3.** Multi Loci Genotypes of Banyuls isolates
- 872 **Supplemental Table1.** Strains used in this study
- 873 **Supplemental Table 2.** Isolation of Bathycoccus strains during 2018/ 2019 winter bloom in
- 874 the Banyuls bay
- 875 **Supplemental Table 3.** Relative abundance of diversity markers in sea water
- 876 **Supplemental data 1.** Sequences and Alignments
- 877 **Supplemental data 2.** Primers used in this study
- 878 **Supplemental Figure 1.** Geographical distribution of TOC1 and CCA1 (Bathy05g02420)
- 879 proteins
- 880 **Supplemental Figure 2.** Abundance of picophytoplankton during winter blooms
- 881 **Supplemental Figure 3.** Images of sea water PCR amplification for yrdC, TOC1 and TIM
- 882 used for Supplemental Table 3
- 883 **Supplemental Figure 4.** Photosynthesis parameters of Mediterranean Bathycoccus strains
- 884

885

Strain	Insertion		Insert 0.2-2kb number	deletion		Coverage
	number	size range		number	size range	
RCC5417	101	36-15979 bp	36	80	50-19025bp	x9
RCC1613	149	51-18972 bp	37	67	50-13730 bp	x239
RCC685	116	51-16349 bp	60	69	51-19026 bp	x52
RCC1615	62	72-4620 bp	23	69	73-13730 bp	x4
RCC1868	49	50-5509 bp	22	43	51-13732 bp	x19
RCC4222	14	76-3011 bp	11	5	51-3999 bp	x30
RCC4752	53	50-15411 bp	34	60	50-13730 bp	x14
mean*	88		35			
*without RCC4222						
INDEL within alignment						

886

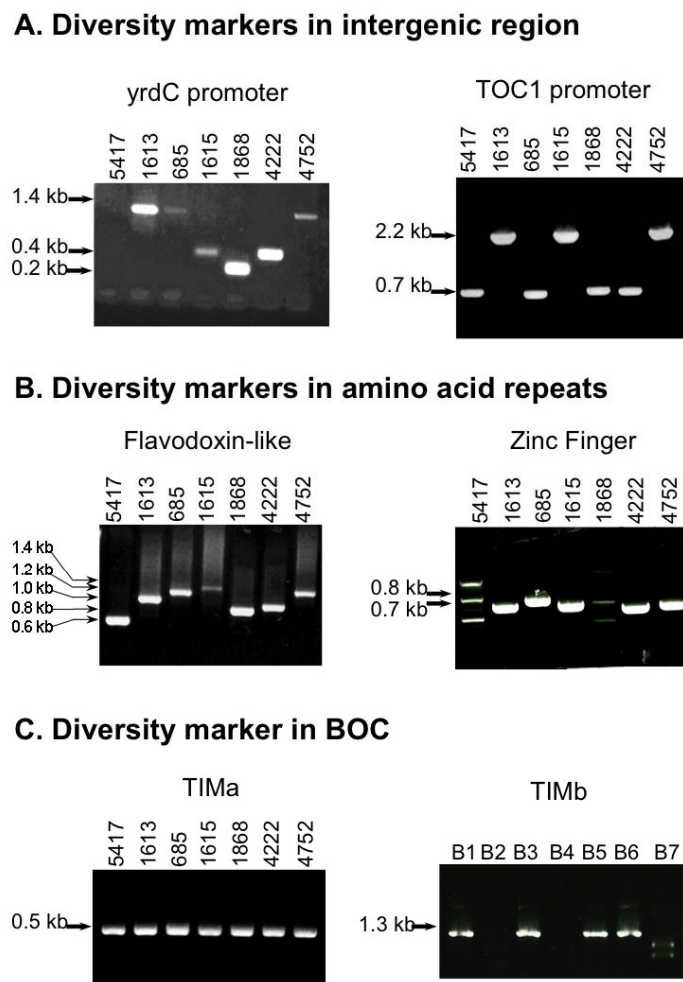
887

Isolates	yrCD prom chr1 primers	TOC1 prom chr17	Flavodoxin chr3	Zinc finger chr15	TiMa chr14
	MDB33+MDB34	MDB7+MDB9	MDB40+MDB41	MDB68+MDB69	MDB57+MDB58
RCC4222	400 bp	700 bp	800 bp	730 bp	530bp
RCC5417	1400 bp	700 bp	600 bp	900 bp	530bp
RCC1613	1400 bp	2.2 kb	1000 bp	730 bp	530bp
RCC685	1400 bp	700 bp	1200 bp	820 bp	530bp
RCC1615	400 bp	2.2 kb	1400 bp	730 bp	530bp
RCC1868	200 bp	700 bp	800 bp	730 bp	530bp
RCC4752	1400 bp	2.2 kb	1200 bp	730 bp	530bp
	3 size variants	2 size variants	5 size variants	3 size variants	1 size variant
	14.28% (200 bp)	42.86% (2.2 kb)	28.57% (1.2 kb)	71.5% (730 bp)	100% (530 bp)

Table 3. Multi Loci Genotypes (MLG) of Banyuls isol								
	Chr1	Chr17	Chr3	Chr15	chr14			
Strains	yrclD prom	TOC1 prom	flavodoxin	C2H2	TIMa			
4222 Banyuls	400bp	700bp	800bp	730 bp	530bp			
4752 Naples	1.4kb	2.2kb	1200bp	730 bp	530bp			
Banyuls 18/19								
MLG 1	200bp	2.2 kb	1200bp	730 bp	530bp	29 strains	5/9 samplings	53%
MLG 2	200bp	2.2kb	1200bp	730 bp	0	16 strains	5/9 samplings	29%
MLG 3	200bp	2.2 kb	800bp	730 bp	530bp	4 strains	3/9 samplings	8%
MLG 4	200bp	700 bp	1200bp	730 bp	530bp	2 strains	2/9 samplings	4%
MLG 5	200bp	2.2kb	1200bp	820 bp	0	1 strain	1/9 samplings	2%
MLG 6	200bp	700 bp	1200bp	820 bp	0	1 strain	1/9 samplings	2%
MLG 7	400bp	700 bp	1400bp	820 bp	530bp	1 strain	1/9 samplings	2%
MLG 8	200bp	2.2kb	1600bp	730 bp	530bp	1 strain	1/9 samplings	2%
Mediterranean								
Size number	2*	2	4	2	2			
Frequency	98% (200bp)	91% (2.2 kb)	89% (1.2kb)	95% (730 bp)	66% (530 bp)			
Globally dispersed								
Size number	3	2	4	3	1			
Frequency	14.28% (200 bp)	42.86% (2.2 kb)	14.28% (1.2 kb)	71.5% (730 bp)	100% (530 bp)			
* no insertion of ANK gene tested with MDB33+MDB35								
similar to RCC4222								
similar to RCC 4752								

888

889 **Figure 1.** Diversity markers among world-wide accessions
890 Samples are arranged on a latitudinal gradient from Arctic (RCC5417) to Mediterranean
891 (RCC4750) sea. The primers used for amplification are specified at the top of the gel. Arrows
892 indicate the size of the various fragments. In 1C TIMb, B1-B7 are 7 seven Bathycoccus
893 isolates from Banyuls during winter 2018/2019.
894
895

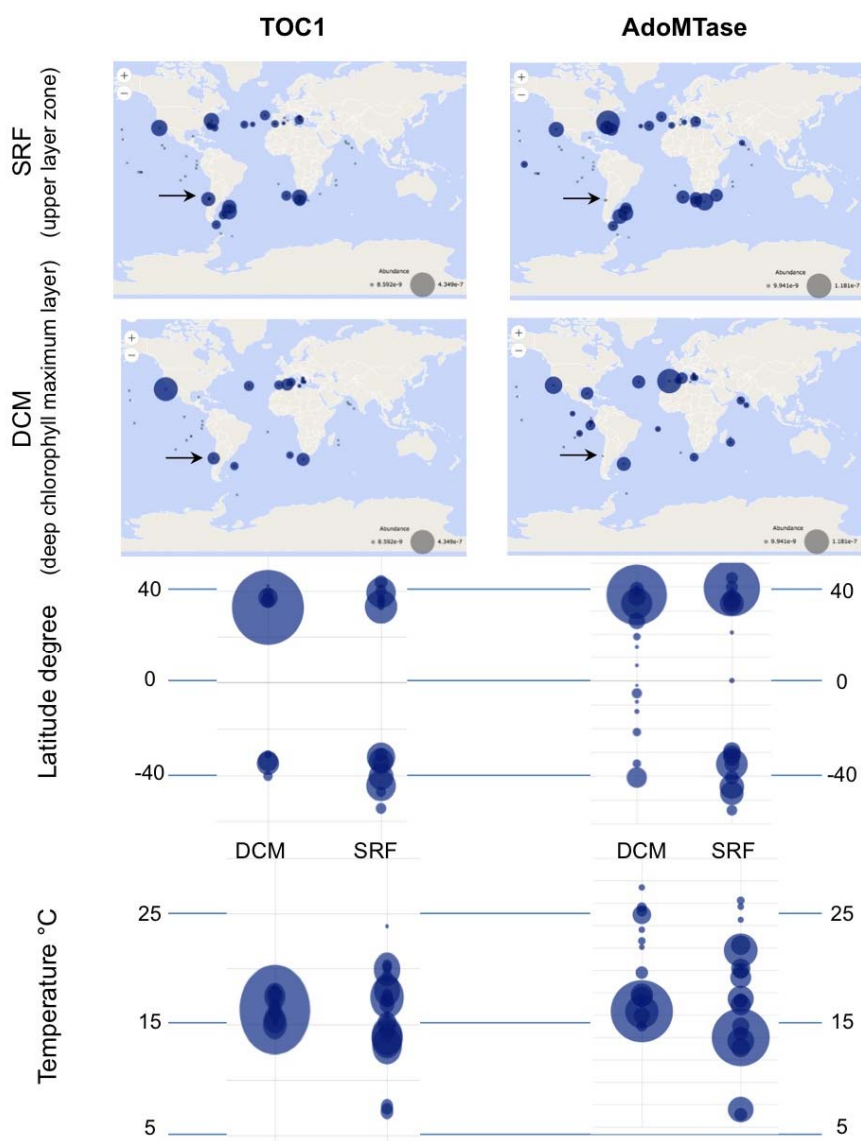


896 **Figure 1. Diversity markers world-wide accessions**

897

898 **Figure 2.** Geographical distribution of TOC1 and AdoMTase proteins

899 The protein sequences of TOC1 and AdoMTase were used as a query at high stringency in
900 OGA. Under these conditions, a single hit was found and its presence and abundance are
901 represented on the world map at surface upper water (SRF) and dense chlorophyll maximum
902 layer (DCM) and in relation to latitude and temperature. The arrows point to a station at the
903 Chilean coast where TOC1 is present but not AdoMTase.



904 **Figure 2 : Geographical distribution of TOC1 and AdoMTase proteins**

905 **Figure 3.** Abundance of phytoplankton during three successive blooms
 906 Seawater at SOLA buoy (Banyuls) was sampled at a depth of 3 meter. After passage on 3 μm
 907 filter, the flow through was analysed by flow cytometry. At each sampling time, the
 908 phytoplankton was categorised and quantified in function of cell size (pico- and nano-
 909 phytoplankton, cyano-bacteria) with indication of the seawater temperature. The mean
 910 seawater temperatures in the three years were in December 15.9°C in 2018, 14.8°C in 2019
 911 and 14.7°C in 2020, in January/February 11.6°C in 2019, 12.8°C in 2020 and 11.8°C in 2021,
 912 in March/April 12.8°C in 2019, 12.2°C in 2020 and 12.8°C in 2021. The main peak of
 913 picophytoplankton abundance was in December 3th 2018 and February 19th 2019, January 7th
 914 and February 11th 2020, January 27th and March 2nd 2021. The most striking difference
 915 between the three years was the sudden abundance in nanophytoplankton in March 2021.

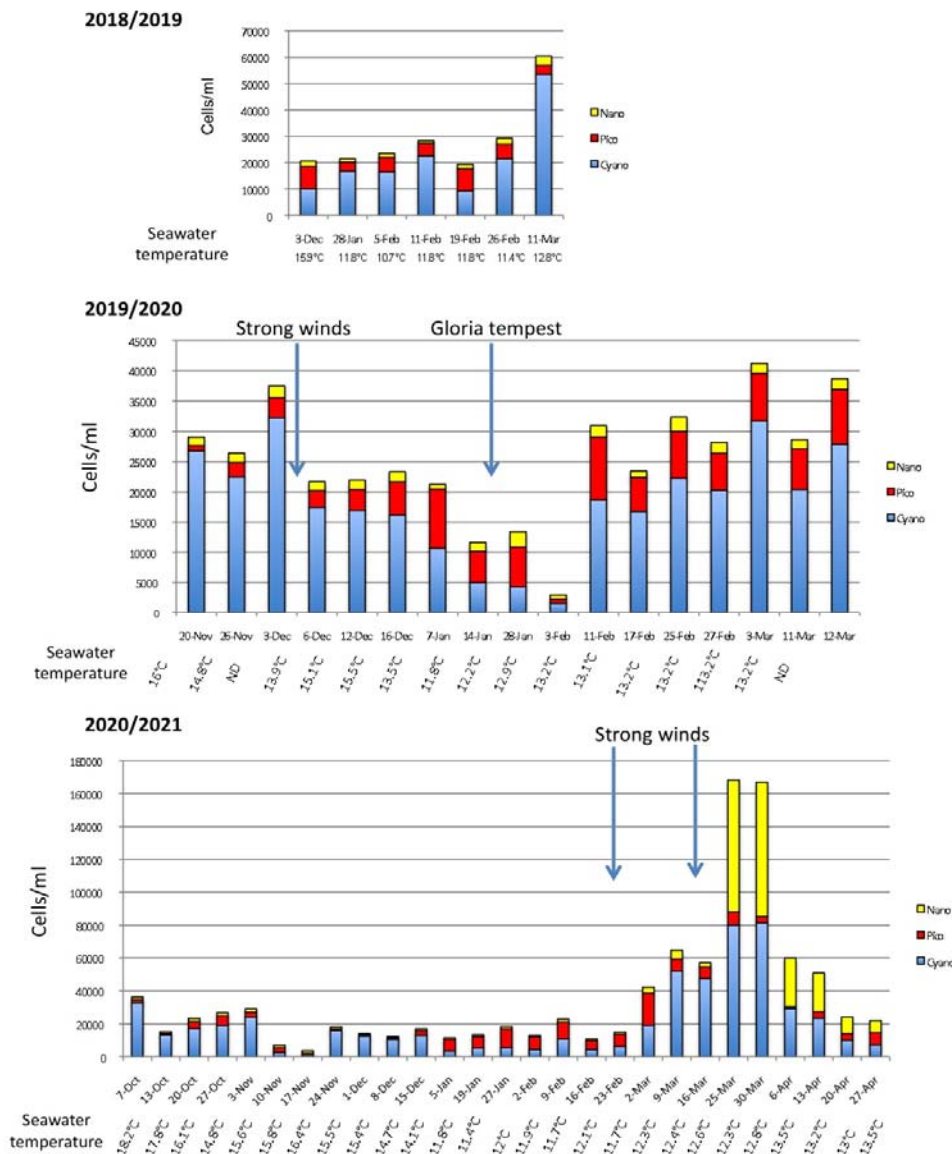


Figure 3. Abundance of phytoplankton during three successive blooms

916

917

918 **Figure 4.** Distribution and abundance of TIM variant proteins in MetaG database
919 A. Phylogenetic tree of TIM proteins from world-wide and Banyuls isolates presenting two
920 main clades each containing one TARA OGA hit, OGATIM4222 or OGATIMA8.
921 OGATIM4222 was retrieved after a query with the TIM protein from RCC4222 and
922 OGATIMA8 with the variant TIM protein in the A8 isolate.
923 B. Geographical presence of TIM variants in OGA. The presence and abundance of each
924 variant is represented in SRF and DCM samples with their correlation to the temperature and
925 latitude parameters.

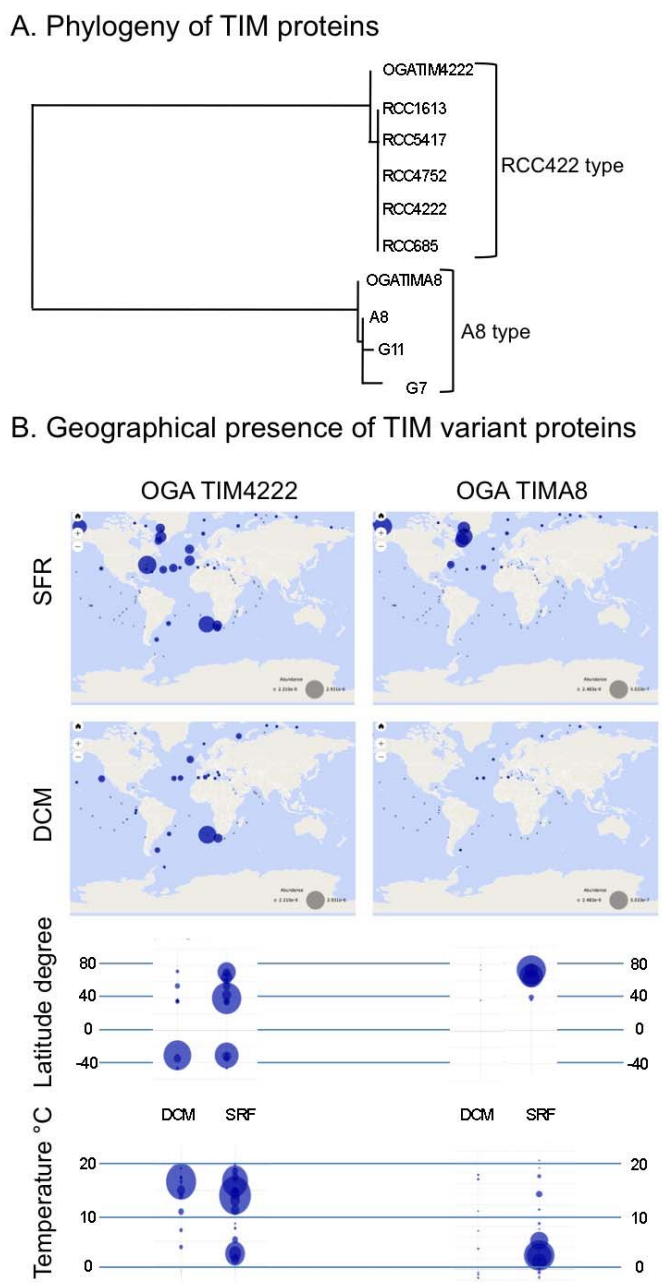


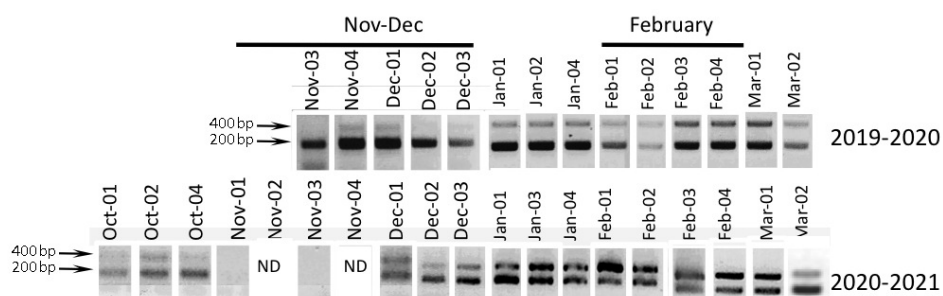
Figure 4. Distribution and abundance of TIM variant proteins in MetaG database

927 **Figure 5. Diversity markers in seawater**

928 For clarity, only extracts are presented in this Figure. The complete set of results is available
 929 in Supplemental Figure3 and Supplemental Table3.

930 Seawater was filtered in autumn from end of November in 2019 and from October 2020. The
 931 relative abundance of the 2 allelic variants of yrdC (200 bp, a deletion or 400 bp, the
 932 reference type) and TIMa and b (absence or presence) were recorded. The onsets of the bloom
 933 were different both their chronology and their population diversity. ND : not determined.

Marker chromosome 1 : yrdC promoter



Marker chromosome 14 : TIM

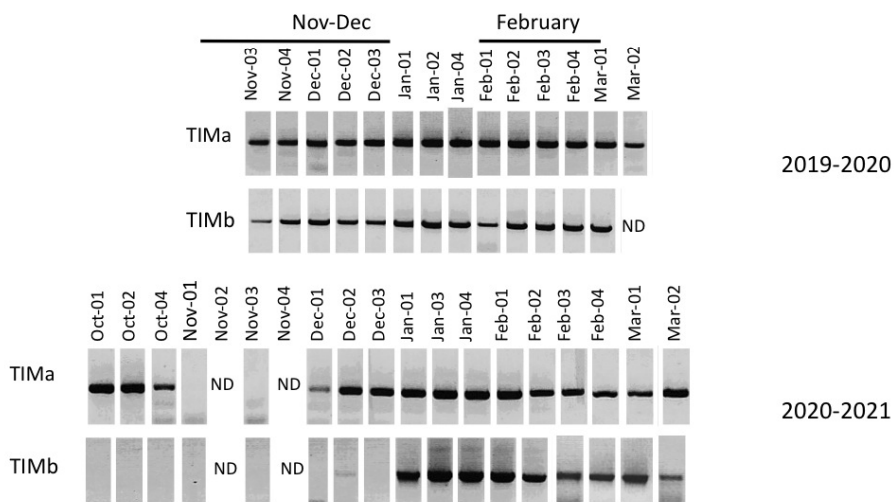


Figure 5. Diversity markers in seawater

934

935 **Figure 6.** Growth of Mediterranean Bathycoccus isolates

936 The growth curve of the “December” and “February” Bathycoccus isolates was determined
937 under 4 different conditions by sampling every day for 9 days. Cell concentration was
938 determined by flow cytometry and is expressed as 10^6 cells/ml.

939

940

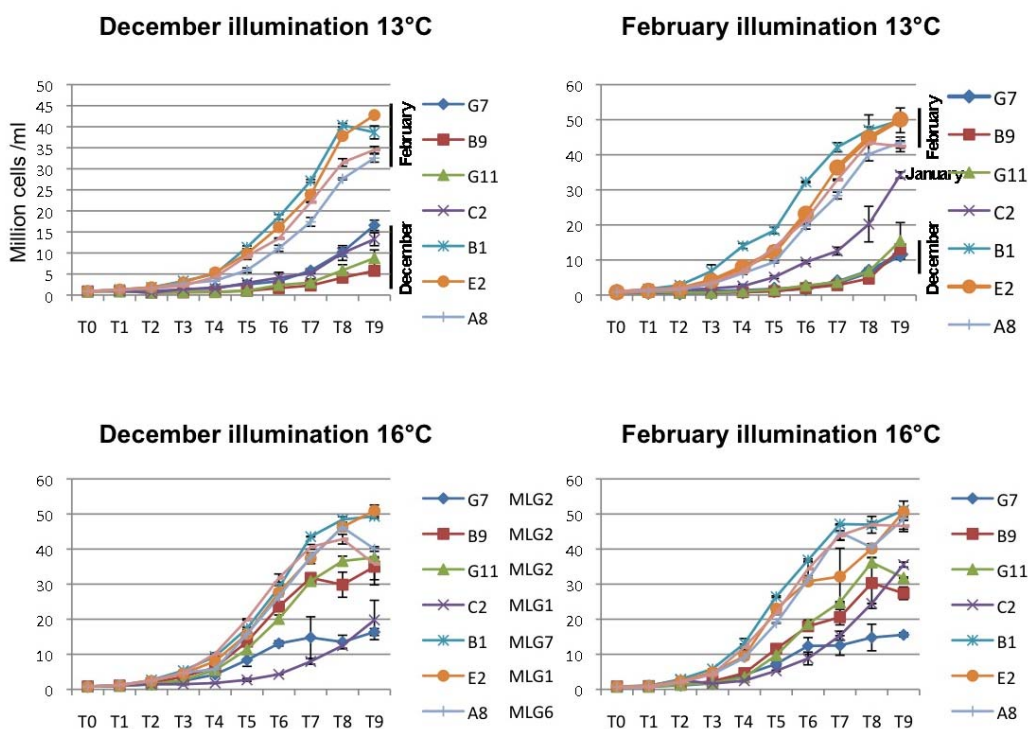


Figure 6 : Growth of Mediterranean Bathycoccus isolates

941

942

943 **Figure 7.** Presence of two additional *Bathycoccus* species in Banyuls bay
 944 A. Alignment of ITS2 nucleotide sequences from B1 (RCC4752, B2 (RCC716) and B3 (C3) strains
 945 and B4 from sea water samples in Kara sea (Belevich et al. 2021).
 946 B. Presence of *Bathycoccus* B2 and B3 type in Banyuls seawater. Primers specific to B2 genome were
 947 derived from TOC1 promoter and intein (Monier et al. 2013) in RCC716 and primers specific to B3
 948 were designed from non-conserved sequences of TOC1 ORF in the C3 isolate. They were used on
 949 seawater samples from 2019 and tested for their specificity on isolated DNA from B1, B2 and B3
 950 strains.
 951 C. Ultrastructure of *Bathycoccus catiminus* B3 type
 952 Transmission electron microscopy image of (a) a B1 Banyuls isolate, (b) a B3 Banyuls isolate and (c)
 953 a close up of detached spider web scales from B3 type *Bathycoccus*. N: nucleus, Cp: chloroplast, St:
 954 starch granule, Sc: scale. Bar = 100 nm.
 955

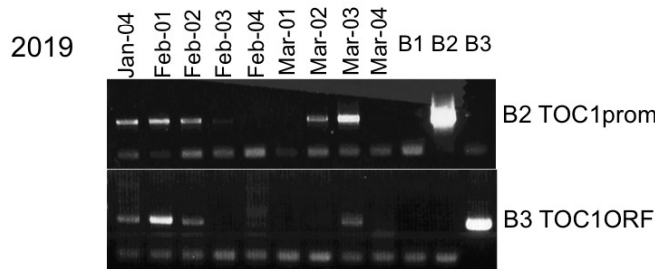
A. ITS2 Alignment

```

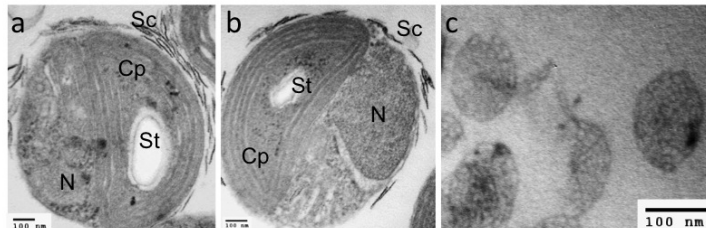
B1 TGTCFCCTCACCTCACTT-TTATTTT-----TGAGCGTGGATCTGGCGTCCGGAA
B2 TGTCFCCTCACCTCCTCCT-----T-----TGAGCGTGGATCTGGCGTCCGGAA
B3 TGTCFCCTCACCTCACCT-TTATTGTATAAGGTACGAGCGTGGATCTGGCGTCCGGAG
B4 TGTCFCCTCACCTCCTCTATTATTGATTTTAAATAAAGAGGTGGATATGGCGTCCGGAA
*****
B1 TCTTTTGTFFTA---TTGAAAGA-CTCGGGTGCCTGAAAACAGTCGTACGTGCGACT
B2 TCTTTCGATTTT---TAGAAAGA-CTCGGGTGCCTGAAAACAGTCGTACGTGCGACT
B3 TCTTTCGATATAATTTGAAAGA-CTCGGGTGCCTGAAAACAGTCGTACGTGCGACT
B4 CATATTGTGTGTA AAAACAACAGTTTCGKGTGCGCTGAAAATAGTCGTACGTGCGACT
***
B1 GTCGCATAACCAACGTGGTAGACCACTCCGGTGGACGATCG-TTCGGTTTGACAGTTGTT
B2 GTCGCACAACCAACGTGGTAGACCACTCCGGTGGACGATCG-TTCGGTTTGACAGTTGTT
B3 GTCGCATAACCAACGTGGTAGACCACTCCGGTGGACGATCG-TTCGGTTTGACAGTTGTT
B4 GTCGCACAACCAACGTGGTAGACCACTCCGGTGGACGATCG-TTCGGTTTGACAGTTGAT
*****
B1 TACCTAAGTATGATCTCGACCG-AATTTATTTCCGT-GTCGAAACCTGTGCTTTTTCAT
B2 TACCTAAGTATGATCTCGGCG-AATTCATCTTCGC-GTCGAAACCTGTGCTTTTTCAT
B3 TACCTAAGTATGATCTCGACCG-AATTGACTTTCGCTGTCGAAACCGTGTGCTTTTTCAT
B4 TACTTA-GTACGATCTCGCTTTCGATTAAATTTATCGAGCGAAACAGTGTGCTTTATGAC
***
B1 CCGCACTTTTCTT-TCACAAGAAAGAGAGCAAAACAAAAGCTTCAC
B2 CCGCACTTTCATCTTGTAAATGCGAGGCGCACCAAGGAAAGCTTCAC
B3 ---CACTTTCCT-TCATCGAAAAGAGTAC---CCAAAAGCTTCAC
B4 T-----CTGTTTATT-TTATTATAACAGGAC----ATAAATGCTTCAC
***

```

B. Presence of *Bathycoccus* B2 and B3 type in Banyuls seawater



C. Ultrastructure of *Bathycoccus catiminus* B3 type



956 **Figure 7.** Presence of two additional *Bathycoccus* species in Banyuls bay